A positive and asymptotic preserving scheme for the linear transport equation on two dimensional unstructured meshes

Clément Lasuen

A positive and asymptotic preserving scheme for the linear transport equation on two dimensional unstructured meshes

Clément Lasuen[1]

[1]CEA, DAM, DIF, F-91297 Arpajon, France

clement.lasuen@gmail.com

November 28, 2023

Abstract

In this paper, we propose a finite volume scheme for the linear transport equation in two space dimensions. This scheme is based on an upwind scheme where the velocity is modified so as to recover the correct diffusion limit. The resulting scheme is *asymptotic preserving*, positive under a classical CFL condition and conservative. Besides, we propose two versions of this scheme that are first and second order consistent on unstructured polygonal meshes.

Contents

1 Introduction

In this work, we propose a finite volume scheme that discretises the radiative transfer equation (see [1]):

$$\frac{1}{c}\partial_t I + \text{div}\ (I\boldsymbol{\omega}) + \sigma^t I = \sigma^s \frac{1}{4\pi}\int_{\mathcal{S}^2} I d\boldsymbol{\omega}' + q. \tag{1}$$

It is a linear Boltzmann type equation. The unknown $I = I(t, \mathbf{x}, \boldsymbol{\omega})$ is the radiative intensity and gives the distribution of photons. It depends on the time variable $t \geq 0$, on the space variable $\mathbf{x} \in \Omega \subset \mathbb{R}^3$ (Ω being the computational domain) and direction $\boldsymbol{\omega} \in \mathcal{S}$, where $\mathcal{S}$ is the unit sphere in $\mathbb{R}^3$. The source term $q = q(t, \mathbf{x}, \boldsymbol{\omega}) \geq 0$ is nonnegative. The scattering cross section is $\sigma^s \geq 0$ and the total cross section is $\sigma^t \geq \sigma^s$. The difference $\sigma^t - \sigma^s$ gives the absorption cross section. We assume here that the speed of light c is equal to 1.

Equation (1) is of great importance in the numerical simulation of inertial confinement fusion (ICF). In these experiments, a small ball of hydrogen (the target) is submitted to intense radiation by laser beams. These laser beams are either pointed directly to the target (direct drive approach), or pointed to gold walls of a hohlraum in which the target is located (indirect drive approach, see Figure 1). These gold walls heat up, emitting X-rays toward the target. The outer layers of the target are heated up, hence ablated. By momentum conservation, the inner part of the target implodes (this is usually called the rocket effect). Hence, the pressure and temperature of the hydrogen inside the target increase, hopefully reaching the thermodynamical conditions for nuclear fusion. This process is summarized in Figure 2. Other possible applications of (1) are radiation hydrodynamics in stellar atmospheres. Of course, the model (1) is over-simplified for these applications as it should, among other things, include a dependence on the frequency. But (1) should be seen as an elementary building block for more realistic models.

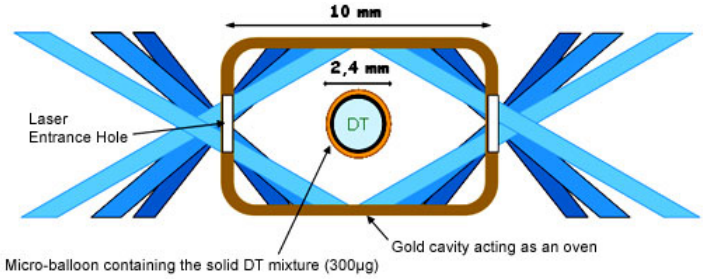

Figure 1: Schematic view of the Hohlraum and the target

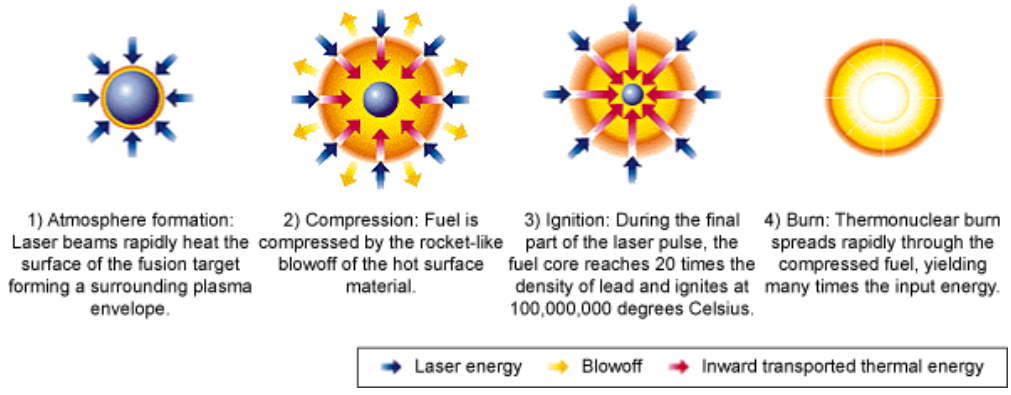

Figure 2: The concept of ICF (inertial confinement fusion) taken from http://www.lanl.gov/projects/dense-plasma-theory/background/dense-laboratory-plasmas.php

It has been shown in [2] that if $q > 0$ and $\sigma^t > 0$ and $\sigma^t - \sigma^s > 0$ then the solution I is positive. Moreover, in [3] the author proved that if $q = 0$ and $\sigma^t = \sigma^s$ then the solution satisfies a maximum principle property.

Eventually, Equation (1) admits a diffusion limit. Let $\varepsilon > 0$ be given. If we replace $\sigma^t \leftarrow \sigma^t/\varepsilon$, $\sigma^s \leftarrow \sigma^s/\varepsilon$ and if we perform the following scaling $t \leftarrow \varepsilon t$, then (1) reads as:

$$\partial_t I + \frac{1}{\varepsilon}\text{div } (I\boldsymbol{\omega}) + \frac{\sigma^t}{\varepsilon^2} I = \frac{\sigma^s}{\varepsilon^2}\frac{1}{4\pi}\int_{\mathcal{S}^2} I d\boldsymbol{\omega}' + \frac{q}{\varepsilon}. \tag{2}$$

Moreover, if $q = 0$ and $\sigma^t - \sigma^s = o(\varepsilon^2)$ then the solution I of (2) converges toward the solution of a diffusion equation $I \xrightarrow[\varepsilon\to 0]{} E^0$ where:

$$\partial_t E^0 - \text{div } \left(\frac{1}{3\sigma^s}\nabla E^0\right) = 0. \tag{3}$$

See [4] [5] [1] for instance. Therefore it is important for a numerical scheme that discretises (2) to be consistent with the limit model (3). In this case, we say that the scheme is *asymptotic-preserving*. The very first works in this direction were [6] and [7]. These papers were dedicated to $1D$ calculations. Some extensions in two or three dimensions on unstructured meshes were proposed and were based on the discontinuous finite element methods (see [8] [9] [10]). More recent works are based on finite volume methods ([11] and [12] which are based on [13] [14]). Lastly [15] proposes an AP finite volume scheme that is based on a micro-macro decomposition.

In this paper, we perform an angular discretisation of (2). We choose K directions $(\boldsymbol{\omega}_k)_{1\leq k\leq K}$ and we define $I_k = I(t, \mathbf{x}, \boldsymbol{\omega}_k)$ for $1 \leq k \leq K$. The integral over the unit sphere in (2) is discretised using a quadrature of *Equal Weights* (see [16]):

$$\frac{1}{4\pi}\int_{\mathcal{S}^2} I d\boldsymbol{\omega}' \approx \frac{1}{K}\sum_{k'=1}^{K} I_{k'}.$$

The quadrature weights are constant and equal to $1/K$ and the directions $(\boldsymbol{\omega}_k)_{1\leq k\leq K}$ satisfy:

$$\frac{1}{K}\sum_{k'=1}^{K}\boldsymbol{\omega}_{k'} = 0, \qquad \frac{1}{K}\sum_{k'=1}^{K}\boldsymbol{\omega}_{k'}\otimes\boldsymbol{\omega}_{k'} = \frac{1}{3}i_3. \tag{4}$$

The matrix i_3 is the identity matrix of size 3. As explained in [16], the number of directions K has to be of the following form $K = 4N^2$ with $N \in \mathbb{N}$. The equation we solve therefore reads as:

$$\partial_t I_k + \frac{1}{\varepsilon}\text{div } (I_k\boldsymbol{\omega}_k) + \frac{\sigma^t}{\varepsilon^2} I_k = \frac{\sigma^s}{\varepsilon^2}\frac{1}{K}\sum_{k'=1}^{K} I_{k'} + \frac{q_k}{\varepsilon}. \tag{5}$$

Moreover, owing to (4), if $q = 0$ and $\sigma^t - \sigma^s = o(\varepsilon^2)$, then Equation (5) admits a diffusion limit: $I_k \xrightarrow[\varepsilon\to 0]{} E^0$ where E^0 is solution to (3). Besides, owing to [17], Equation (3) satisfies a positivity principle and we can write it as:

$$\partial_t E^0 - \text{div } \left(E^0\frac{\nabla E^0}{3\sigma^s E^0}\right) = 0. \tag{6}$$

In this work, we focus on the two dimensional case. Beside, the method we present uses the reformulation (6) and has the following properties:

- asymptotic preserving: the scheme we obtain when $\varepsilon \to 0$ is consistent with (3),
- consistent on unstructured $2D$ meshes in any regime. We propose a scheme that is first order consistent and another one that is second order consistent,
- positivity preserving: if at iteration n the numerical solution is positive (resp nonnegative), then the solution at iteration $n + 1$ is also positive (resp nonnegative) possibly under a CFL condition,
- conservative.

The main idea of our method is to use an upwind scheme to discretise Equation (5) and to modify the streaming velocity in order to obtain a scheme that is consistent with (6) when $\varepsilon \to 0$. The scheme is said to be *composite* as the fluxes are computed at the nodes and at the edges of the cells (this idea was first introduced in [18, 14]).
The article is organized as follows. In Section 2, we define the notations that we use in the rest of the paper and we explain the geometrical assumptions we need to develop our method. In Section 3 we present a first order consistent scheme. Section 4 is dedicated to the second order scheme. Numerical examples are shown in Section 5. Eventually, our method being based on an upwind scheme, we present it and we detail its properties in Appendix 6.

2 Notations assumptions on the mesh

We present here some notations that will be used in the rest of the paper. Let Ω_j be a cell of the mesh $\mathcal{T}$ paving the domain Ω, we define:

- V_j is the volume of the cell Ω_j,
- $(\mathbf{x}_r)_r$ the coordinates of the vertices of the cell j;
- $\sum_{r\in\Omega_j}$ the sum over all the vertices of the cell j;
- $r+1/2$ is the index of the edge between the nodes $\mathbf{x}_r$ and $\mathbf{x}_{r+1}$, its middle is denoted by $\mathbf{x}_{r+1/2} = (\mathbf{x}_r + \mathbf{x}_{r+1})/2$,
- $\sum_{r+1/2\in\Omega_j}$ the sum over all edges of the cell j;
- a *degree of freedom* (denoted as *dof*) is either a node or a mid-edge point;
- $N_j = \sum_{\mathrm{dof}\in\Omega_j} 1$ the number of degrees of freedom in the cell Ω_j;
- $\sum_{i|\mathrm{dof}\in\Omega_i}$ the sum, for a given degree of freedom, over all the cells that contains this degree of freedom;
- $N_r = \sum_{i|r\in\Omega_i} 1$ the number of cells that contains the given node r;
- $\sum_{j\in\mathcal{T}}$ the sum over all the cells of the mesh;
- $J = \sum_{j\in\mathcal{T}} 1$ is the number of cells of the mesh;
- h the maximum length of edges of the mesh;
- $I^n_{k,j}$ is the value of the unknown in direction k, in cell j, at iteration n;
- $I_k = (I_{k,i})_{i\in\mathcal{T}}$ is the vector of the values of the unknown in direction k;
- $E_j = \sum_{k'=1}^{K} I_{k',j}/K$ is the average, in cell j, over the directions;
- $E = (E_i)_{i\in\mathcal{T}}$ is the vector of the averages;
- for $p \in \mathbb{N}^*$, the identity matrix of size p is denoted by i_p;
- $\langle\cdot,\cdot\rangle$ the inner product in $\mathbb{R}^2$;
- $\|\cdot\|$ is the L^∞ norm for vectors, that is to say, for $p \in \mathbb{N}^*$:

$$\forall\, U \in \mathbb{R}^p, \quad \|U\| = \max_{1\le l\le p} |U_i|, \qquad \forall\, A \in \mathbb{R}^{p\times p}, \quad \|A\| = \max_{U\neq 0} \frac{\|AU\|}{\|U\|}.$$

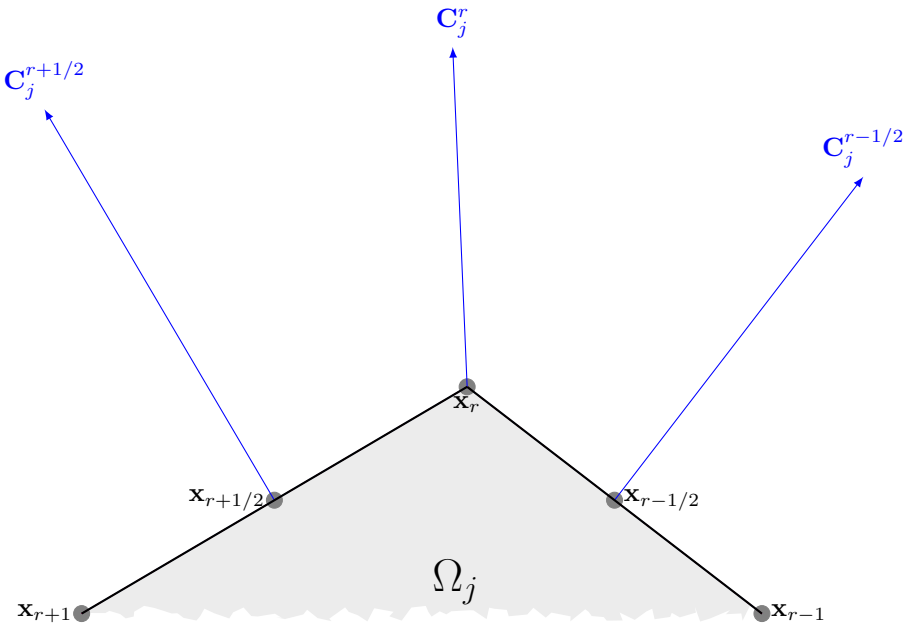

Figure 3: Normal vectors at the nodes and the edges of the cell Ω_j

Let $\mathbf{x}_{r-1}$, $\mathbf{x}_r$ and $\mathbf{x}_{r+1}$ be 3 consecutive nodes of Ω_j (see Figure 3 for instance). The normal vector to the edge $[\mathbf{x}_r, \mathbf{x}_{r+1}]$ is denoted by $\mathbf{C}_j^{r+1/2} = (\mathbf{x}_{r+1} - \mathbf{x}_r)^\perp$, where for any vector $\boldsymbol{\xi} \in \mathbb{R}^2$:

$$\boldsymbol{\xi} = \begin{pmatrix} \xi_1 \\ \xi_2 \end{pmatrix}, \qquad \boldsymbol{\xi}^\perp = \begin{pmatrix} -\xi_2 \\ \xi_1 \end{pmatrix}.$$

Similarly, we define the *normal vector to the node r* as:

$$\mathbf{C}_j^r = \frac{1}{2}(\mathbf{x}_{r+1} - \mathbf{x}_{r-1})^\perp = \frac{1}{2}\left(\mathbf{C}_j^{r+1/2} + \mathbf{C}_j^{r-1/2}\right). \tag{7}$$

Definition (7) was first introduced in [13]. We also define the matrix:

$$\beta_r = \sum_{i|r\in\Omega_i} \mathbf{C}_i^r \otimes (\mathbf{x}_r - \mathbf{x}_i), \tag{8}$$

We assume that there exists a constant C_1 such that, for any *dof* and any cell j:

$$\frac{1}{C_1}h^2 \le V_j \le C_1 h^2, \qquad N_{\text{dof}} \le C_1, \qquad N_j \le C_1, \tag{9}$$

Note that by definition we have $\left\|\mathbf{C}_j^{\text{dof}}\right\| \le h$. Moreover, we assume that for any node $r \in \mathcal{T}$ the matrix β_r defined in (8) is positive definite:

$$\forall \boldsymbol{\xi} \in \mathbb{R}^2,\ \langle \beta_r \boldsymbol{\xi}, \boldsymbol{\xi}\rangle \ge \frac{1}{C_1} h^2 \|\boldsymbol{\xi}\|^2. \tag{10}$$

Thus it is non-singular and we have:

$$\|\beta_r^{-1}\| \le C_1 \frac{1}{h^2}. \tag{11}$$

Assumption (10) is studied in [19]. We have the following result:

Proposition 2.1. *Let r be an inner node, we have:*

$$\sum_{i|r\in\Omega_i} \mathbf{C}_i^r = 0.$$

We also have the following quadrature formula.

Theorem 2.2. *Let $g \in \mathcal{C}^2(\mathbb{R}^2;\mathbb{R})$. We assume Assumptions (9) are fulfilled. Then, for all $\theta \in [0,1]$:*

$$\frac{1}{V_j}\int_{\partial\Omega_j} g\mathbf{n} = \frac{1}{V_j}\left[(1-\theta)\sum_{r\in\Omega_j} g(\mathbf{x}_r)\mathbf{C}_j^r + \theta \sum_{r+1/2\in\Omega_j} g(\mathbf{x}_{r+1/2})\mathbf{C}_j^{r+1/2}\right] + O(h). \tag{12}$$

Moreover, the remainder in (12) vanishes if g is an affine function.

Remark 1. *We propose here some explanations on the choice of the parameter θ:*

- *$\theta = 0$: node based scheme, consistent but may suffer from* cross stencil *phenomena (see [12]),*
- *$\theta = 1$: edge-based scheme, useful to implement boundary conditions (see Section 6.3),*
- *$\theta = 2/3$: better precision. Formula (12) is exact for quadratic functions and the remainder is $O(h^2)$. This choice may allow to have third order convergence (see [20] for instance).*

3 First order scheme

In this Section, we present the construction of our first order scheme.

3.1 Upwind scheme and new streaming velocity

Equation (5) is integrated over the cell Ω_j. We use Theorem 2.2 to approximate the flux:

$$V_j\frac{d}{dt}I_{k,j} + \theta\sum_{r\in j}\left\langle\bar{\boldsymbol{\omega}}_{k,r},\mathbf{C}_j^r\right\rangle\hat{I}_{k,j}^r + (1-\theta)\sum_{r+1/2\in j}\left\langle\bar{\boldsymbol{\omega}}_{k,r+1/2},\mathbf{C}_j^{r+1/2}\right\rangle\hat{I}_{k,j}^{r+1/2} + V_j\frac{\sigma_j^t}{\varepsilon^2}I_{k,j} \tag{13}$$

$$= V_j\frac{\sigma_j^s}{\varepsilon^2}\frac{1}{K}\sum_{k'=1}^{K} I_{k',j} + V_j q_{k,j}. \tag{14}$$

The quantity $\hat{I}_{k,j}^{\mathrm{dof}}$ is an approximation of I at point $\mathbf{x}_{\mathrm{dof}}$ in cell Ω_j. It is computed using an upwind scheme:

$$\hat{I}_{k,j}^{\mathrm{dof}} = \begin{cases} I_{k,j} & \text{if } \langle\bar{\boldsymbol{\omega}}_{k,\mathrm{dof}},\mathbf{C}_j^{\mathrm{dof}}\rangle > 0, \\ \dfrac{1}{\sum_{i\in\mathcal{A}_{\mathrm{dof}}^+}\langle\bar{\boldsymbol{\omega}}_{k,\mathrm{dof}},\mathbf{C}_i^{\mathrm{dof}}\rangle}\displaystyle\sum_{i\in\mathcal{A}_{\mathrm{dof}}^+}\langle\bar{\boldsymbol{\omega}}_{k,\mathrm{dof}},\mathbf{C}_i^{\mathrm{dof}}\rangle I_{k,i} & \text{else,} \end{cases} \tag{15}$$

and: $\mathcal{A}_{\mathrm{dof}}^+ = \{i, \langle\bar{\boldsymbol{\omega}}_{k,\mathrm{dof}},\mathbf{C}_i^{\mathrm{dof}}\rangle > 0\}$. The upwind scheme and its properties are introduced in detail in Section 6. The streaming velocity $\bar{\boldsymbol{\omega}}_{k,\mathrm{dof}}$ is a consistent approximation of $\boldsymbol{\omega}_k/\varepsilon$, meaning that:

$$\bar{\boldsymbol{\omega}}_{k,\mathrm{dof}} \xrightarrow[h\to 0]{} \frac{1}{\varepsilon}\boldsymbol{\omega}_k. \tag{16}$$

Moreover, in order to be consistent with (6), we also impose:

$$\bar{\boldsymbol{\omega}}_{k,\mathrm{dof}} \xrightarrow[\varepsilon\to 0]{} -\frac{\nabla E}{3\sigma_{\mathrm{dof}}^s E}, \tag{17}$$

where E is the average over the directions (see Section 2): $E = \sum_{k'=1}^{K} I_{k'}/K$. The condition (17) is justified in the next sections. Therefore we propose:

$$\bar{\boldsymbol{\omega}}_{k,\mathrm{dof}} = \frac{\varepsilon \boldsymbol{\omega}_k + \sigma^s_{\mathrm{dof}} h^2 \mathbf{u}_{\mathrm{dof}}}{3(\sigma^s_{\mathrm{dof}} h)^2 + \varepsilon^2}. \tag{18}$$

The quantity $\mathbf{u}_{\mathrm{dof}}$ is an approximation of $-\nabla E/E$ at point $\mathbf{x}_{\mathrm{dof}}$ that is given below. Therefore Definition (18) does satisfy (16) and (17). Moreover, in the streaming regime, that is to say when $\sigma^t = \sigma^s = 0$ then we have exactly $\bar{\boldsymbol{\omega}}_{k,\mathrm{dof}} = \boldsymbol{\omega}_k/\varepsilon$. Eventually, $\mathbf{u}_r$ and $\mathbf{u}_{r+1/2}$ are given by:

$$\mathbf{u}_r = \beta_r^{-1} \frac{1}{E_r} \sum_{i|r\in\Omega_i} E_i \mathbf{C}_i^r, \qquad E_r = \frac{1}{N_r} \sum_{i|r\in\Omega_i} E_i + h^2, \qquad \mathbf{u}_{r+1/2} = \frac{\mathbf{u}_r + \mathbf{u}_{r+1}}{2}, \tag{19}$$

where β_r is defined in (8). The coefficient E_r is an approximation of E at point $\mathbf{x}_r$. We add a h^2 term in order to make $\mathbf{u}_r$ well defined in the case where all the $(E_i)_i$ vanish. Moreover, the quantity $\beta_r^{-1} \sum_{i|r\in\Omega_i} E_i \mathbf{C}_i^r$ is an approximation of $-\nabla E$ at point $\mathbf{x}_r$. Indeed, using a Taylor expansion, we easily have:

$$E(\mathbf{x}_r) - E(\mathbf{x}_i) = \langle \nabla E(\mathbf{x}_r), \mathbf{x}_r - \mathbf{x}_i \rangle + O(h^2). \tag{20}$$

Multiplying (20) by $\mathbf{C}_i^r$ and summing around all the neighbouring cells $\{i | r \in \Omega_i\}$ leads to:

$$E(\mathbf{x}_r) \sum_{i|r\in\Omega_i} \mathbf{C}_i^r - \sum_{i|r\in\Omega_i} E(\mathbf{x}_i) \mathbf{C}_i^r = \beta_r \nabla E(\mathbf{x}_r) + O(h^3).$$

Using Proposition 2.1 and (11), we show that $\beta_r^{-1} \sum_{i|r\in\Omega_i} E_i \mathbf{C}_i^r$ is indeed first order consistent with $-\nabla E(\mathbf{x}_r)$:

$$\nabla E(\mathbf{x}_r) = -\beta_r^{-1} \sum_{i|r\in\Omega_i} E(\mathbf{x}_i) \mathbf{C}_i^r + O(h).$$

Eventually, the resulting scheme is nonlinear and first order consistent with (5). We write it more compactly as:

$$V_j \frac{d}{dt} I_{k,j} + \left[M_{k,\varepsilon} I_k \right]_j + V_j \frac{\sigma_j^t}{\varepsilon^2} I_{k,j} = V_j \frac{\sigma_j^s}{\varepsilon^2} \frac{1}{K} \sum_{k'=1}^{K} I_{k',j} + V_j q_{k,j}, \tag{21}$$

where $M_{k,\varepsilon} = M\left((\bar{\boldsymbol{\omega}}_{k,\mathrm{dof}})_{\mathrm{dof}\in\mathcal{T}} \right)$ is the streaming matrix with velocity field $(\bar{\boldsymbol{\omega}}_{k,\mathrm{dof}})_{\mathrm{dof}\in\mathcal{T}}$ and $M(\cdot)$ is defined in (57). We remind that $M_{k,\varepsilon}$ depends on the unknown I_k and on ε.

3.2 Partially implicit time discretisation

We use a partially implicit time discretisation. The streaming velocity is chosen at time t^n while the sources are chosen at time t^{n+1}:

$$V_j \frac{I_{k,j}^{n+1} - I_{k,j}^n}{\Delta t} + \left[M_{k,\varepsilon}^n I_k^{n+1} \right]_j + V_j \frac{\sigma_j^t}{\varepsilon^2} I_{k,j}^{n+1} = V_j \frac{\sigma_j^s}{\varepsilon^2} \frac{1}{K} \sum_{k'=1}^{K} I_{k',j}^{n+1} + V_j q_{k,j}. \tag{22}$$

Even though the scheme (13) is nonlinear, the time discretisation we choose only requires to solve a linear system at each iteration. Moreover, it is is conservative:

Proposition 3.1. *We assume periodic boundary conditions are imposed. If $\sigma_j^t = \sigma_j^s$ and $q = 0$, then the scheme* (13) *is conservative:*

$$\sum_{j\in\mathcal{T}} V_j E_j^{n+1} = \sum_{j\in\mathcal{T}} V_j E_j.$$

Proof. This result is a direct consequence of Proposition 6.1. □

Besides, we can easily prove that the solution of System (22) is positive (Proposition 3.5) as the matrix involved is a strict M-matrix, as defined in Definition 3.2. As stated in Proposition 3.3, the inverses of these matrices have nonnegative entries.

Definition 3.2 (M-matrix)**.** *Let $p \in \mathbb{N}^*$ and A a $p \times p$ matrix. A is an M-matrix if it can be written under the form $A = cI - B$ where B has nonnegative coefficients and its spectral radius $\rho(B)$ satisfies:*

$$\rho(B) \leq c. \tag{23}$$

If (23) *is a strict inequality, then we say that A is a* strict *M-matrix.*

Proposition 3.3. *Let $p \in \mathbb{N}$ and $A \in \mathbb{R}^{p\times p}$ be a strict M-matrix. Then A is nonsingular and its inverse has nonnegative coefficients.*

Proof. The proof can be found in [21]. □

The following proposition is useful in the proof of Proposition 3.5.

Proposition 3.4. *Let $p \in \mathbb{N}^*$ and $A \in \mathbb{R}^{p\times p}$ be such that $A_{l,l'} \leq 0$ if $l \neq l'$ and:*

$$\forall l \leq p, \quad \sum_{l'=1, l'\neq l}^{p} |A_{l,l'}| \leq A_{l,l}. \tag{24}$$

Then A is an M-matrix. Besides, if the inequality (24) *is strict then A is a strict M-matrix.*

Proof. The proof can be found in Appendix 7. □

Proposition 3.5. *If the $\left(I^n_{k,j}\right)_{k,j}$ are nonnegative (resp positive), then the solution of* (22) *$\left(I^{n+1}_{k,j}\right)_{k,j}$ is also nonnegative (resp positive).*

Proof. We write (22) as:

$$I^{n+1}_{k,j}V_j\left(1+\frac{\Delta t}{\varepsilon^2}(\sigma^t_j-\sigma^s_j)+\frac{\sigma^s_j\Delta t}{\varepsilon^2}\left(1-\frac{1}{K}\right)\right)+\Delta t\left[M^n_{k,\varepsilon}I^{n+1}_k\right]_j-V_j\frac{\sigma^s_j\Delta t}{\varepsilon^2}\frac{1}{K}\sum_{k'=1,k'\neq k}^{K}I^{n+1}_{k',j}=V_jI^n_{k,j}+\Delta tV_jq_{k,j}. \tag{25}$$

The matrices $M^n_{k,\varepsilon}$ are M-matrices (see Proposition 6.2). Thus the matrix of System (22) is a strict M-matrix, and according to Proposition 3.3, it is nonsingular and its inverse has nonnegative coefficients. The right hand side of (25) is nonnegative by assumption, therefore the $\left(I^{n+1}_{k,j}\right)_{k,j}$ are nonegative. In addition, every line of the invert of the matrix of System (22) has at least one nonzero entry, if the right hand side is positive then the $\left(I^{n+1}_{k,j}\right)_{k,j}$ are also positive. □

However, System (22) has size $JK \times JK$. In order to solve it, we reformulate it and we use a fixed point procedure that requires the solving of smaller linear systems. We define:

$$\mu^{(1)}_j = \frac{\varepsilon^2}{\varepsilon^2+\Delta t\sigma^t_j}, \qquad \mu^{(2)}_j = \frac{\Delta t\sigma^s_j}{\varepsilon^2+\Delta t\sigma^t_j}\frac{\varepsilon^2}{\varepsilon^2+\Delta t(\sigma^t_j-\sigma^s_j)}. \tag{26}$$

Proposition 3.6. *System (22) is equivalent to:*

$$I^{n+1}_{k,j}+\mu^{(1)}_j\frac{\Delta t}{V_j}\left[M^n_{k,\varepsilon}I^{n+1}_k\right]_j=\mu^{(1)}_jI^n_{k,j}+\mu^{(2)}_j\frac{1}{K}\sum_{k'=1}^{K}I^n_{k',j}-\mu^{(2)}_j\frac{\Delta t}{V_j}\frac{1}{K}\sum_{k'=1}^{K}\left[M^n_{k',\varepsilon}I^{n+1}_{k'}\right]_j \tag{27}$$

$$+\Delta t\left(\mu^{(1)}_jq_{k,j}+\mu^{(2)}_j\frac{1}{K}\sum_{k'=1}^{K}q_{k',j}\right).$$

Proof. $\Longrightarrow$ Summing (22) over the directions leads to:

$$\frac{1}{K}\sum_{k'=1}^{K} I_{k',j}^{n+1} = \nu\frac{1}{K}\sum_{k'=1}^{K}\left(I_{k',j}^{n} - \frac{\Delta t}{V_j}\left[M_{k',\varepsilon}^{n} I_{k'}^{n+1}\right]_j\right) + \nu\Delta t\frac{1}{K}\sum_{k'=1}^{K} q_{k',j}, \tag{28}$$

where ν is given by:

$$\nu = \frac{\varepsilon^2}{\varepsilon^2 + \Delta t(\sigma_j^t - \sigma_j^s)}. \tag{29}$$

Moreover, using Equation (26), Equation (22) can be written as:

$$I_{k,j}^{n+1} + \mu_j^{(1)}\frac{\Delta t}{V_j}\left[M_{k,\varepsilon}^{n} I_k^{n+1}\right]_j = \mu_j^{(1)} I_{k',j}^{n} + \mu_j^{(1)}\Delta t q_j + \frac{\Delta t\sigma_j^s}{\varepsilon^2 + \Delta t\sigma_j^t}\frac{1}{K}\sum_{k'=1}^{K} I_{k',j}^{n+1} \tag{30}$$

Inserting (28) into (30) gives (27).
$\Longleftarrow$ Summing (27) over the directions and using (4) gives:

$$\frac{1}{K}\sum_{k'=1}^{K} I_{k',j}^{n+1} + \left(\mu_j^{(1)} + \mu_j^{(2)}\right)\frac{\Delta t}{V_j}\frac{1}{K}\sum_{k'=1}^{K}\left[M_{k,\varepsilon}^{n} I_k^{n+1}\right]_j = \left(\mu_j^{(1)} + \mu_j^{(2)}\right)\frac{1}{K}\sum_{k'=1}^{K} I_{k',j}^{n} + \Delta t\left(\mu_j^{(1)} + \mu_j^{(2)}\right)\frac{1}{K}\sum_{k'=1}^{K} q_{k',j}. \tag{31}$$

Using (29) and (26), one has $\mu_j^{(1)} + \mu_j^{(2)} = \nu$. Therefore (31) gives (28), which implies (22).

□

This reformulation (27) allows to prove the AP property of our scheme. Indeed, choosing $\sigma_j^t = \sigma_j^s$ and $\varepsilon = 0$ in (27) leads to:

$$I_{k,j}^{n+1} = \left(\frac{1}{K}\sum_{k'=1}^{K} I_{k',j}^{n}\right) - \frac{\Delta t}{V_j}\frac{1}{K}\sum_{k'=1}^{K}\left[M_{k',0}^{n} I_{k'}^{n+1}\right]_j + \Delta t\frac{1}{K}\sum_{k'=1}^{K} q_{k',j}.$$

Moreover, noticing that $M_{k',0} = M\left(\frac{1}{3\sigma^s}\mathbf{u}\right)$ does not depend on the direction k, we deduce that $I_{k,j}^{n+1}$ does not depend on k either. The limit scheme consequently reads as:

$$I_{k,j}^{n+1} = \frac{1}{K}\sum_{k'=1}^{K} I_{k,j}^{n+1} = \left(\frac{1}{K}\sum_{k'=1}^{K} I_{k',j}^{n}\right) - \frac{\Delta t}{V_j}\left[M\left(\frac{1}{3\sigma^s}\mathbf{u}^n\right)\left(\frac{1}{K}\sum_{k'=1}^{K} I_{k'}^{n+1}\right)\right]_j + \Delta t\frac{1}{K}\sum_{k'=1}^{K} q_{k',j}. \tag{32}$$

In addition, as the matrix $M\left(\frac{1}{3\sigma^s}\mathbf{u}\right)$ discretises a streaming equation with velocity field $\frac{1}{3\sigma^s}\mathbf{u}$ and reminding that the latter is a consistent approximation of $-\nabla E/(3\sigma^s E)$, we deduce that (32) is consistent with (6).

3.3 Solving System (30) with a fixed point algorithm

In order to solve the "big" system of size $JK \times JK$ (30), we use a fixed point algorithm and we iterate on the source term:

$$I_{k,j}^{n+1,l+1} + \mu_j^{(1)}\frac{\Delta t}{V_j}\left[M_{k,\varepsilon}^{n} I_k^{n+1,l+1}\right]_j = \mu_j^{(1)} I_{k,j}^{n} + \mu_j^{(2)}\frac{1}{K}\sum_{k'=1}^{K} I_{k',j}^{n} - \mu_j^{(2)}\frac{\Delta t}{V_j}\frac{1}{K}\sum_{k'=1}^{K}\left[M_{k',\varepsilon}^{n} I_{k'}^{n+1,l}\right]_j \tag{33}$$

$$+\Delta t\left(\mu_j^{(1)} q_{k,j} + \mu_j^{(2)}\frac{1}{K}\sum_{k'=1}^{K} q_{k',j}\right).$$

At each sub-iteration, we have K linear systems to solve (this step can be paralelized). The rest of this section is devoted to the analysis of the fixed point strategy. In the end we find a condition on Δt that

ensures the convergence of the sequence $\left(\left[I^l_{k,j}\right]_{k,j}\right)_{l\in\mathbb{N}}$ defined in (33) toward the solution of (30). This result is given in Theorem 3.11. Equation (33) can be set under the following form:

$$f\left(X^{l+1}\right) = X^l, \qquad X^l \in \mathbb{R}^{JK}, \qquad X^l_{kJ+j} = I^{n+1,l}_{k,j}. \tag{34}$$

The function f is defined by:

$$f(X) = \left[i_{JK} + \Delta t \mu^{(1)} \bar{M}\right]^{-1} \left(B + \Delta t \mu^{(2)} \bar{C}\bar{M}X\right), \tag{35}$$

where $\bar{M}$ and $\bar{C}$ are $(JK)\times(JK)$ matrices:

$$\bar{C}_{kJ+j,k'J+j'} = \frac{1}{K} 1_{k=k'}, \qquad \bar{M} = \operatorname{diag}\left(S^{-1}M_{1,\varepsilon},\ \ldots\ , S^{-1}M_{K,\varepsilon}\right). \tag{36}$$

The matrix $S^{-1} = \operatorname{diag}\left((V_j^{-1})_{j\in\mathcal{T}}\right)$ is the matrix of the inverse of the areas of the cells and $\mu^{(1)} = \operatorname{diag}\left((\mu^{(1)}_j)_{j\in\mathcal{T}}\right)$. The vector B is given by:

$$B_{kJ+j} = \mu^{(1)}_j I^n_{k,j} + \Delta t \left(\mu^{(1)}_j q_{k,j} + \mu^{(2)}_j \frac{1}{K}\sum_{k'=1}^{K} q_{k',j}\right) + \mu^{(2)}_j \frac{1}{K}\sum_{k'=1}^{K} I^n_{k',j}. \tag{37}$$

The gradient of f is equal to:

$$\nabla f(X) = \Delta t \mu^{(2)} \left[i_{JK} + \Delta t \mu^{(1)} \bar{M}\right]^{-1} \bar{C}\bar{M}. \tag{38}$$

Our aim is to find a condition on Δt that makes the gradient (38) smaller than 1, thus making f a contraction mapping. Lemmas 3.7 3.8 3.9 3.10 allow to give an upper bound on the matrix $\left[i_{JK} + \Delta t \mu^{(1)} \bar{M}\right]^{-1}$. Theorem 3.11 gives a condition on Δt for the fixed point procedure to converge. We emphasize that this condition does not becomes $\Delta t = O(\varepsilon)$. That is to say, our fixed point procedure converges in the diffusion regime and no acceleration procedure is necessary.

Lemma 3.7. *Under Assumptions* (9) (10) (11)*, and assuming that the* $(I_{k,j})_{k\leq K, j\in\mathcal{T}}$ *are nonnegative, there exists a constant such that, for any* dof*:*

$$\|\mathbf{u}_{dof}\| \leq \frac{C_{3.6}}{h}.$$

Proof. As the $(I_{k,j})_{k\leq K, j\in\mathcal{T}}$ are nonnegative, the $(E_j)_{j\in\mathcal{T}}$ are also nonnegative and we have:

$$\frac{E_i}{E_r} \leq N_r \leq C_1.$$

Therefore, using Assumption (9) we have:

$$\left\| \frac{1}{E_r} \sum_{i|r\in\Omega_i} E_i \mathbf{C}^r_i \right\| \leq C_1^2 h.$$

Using (11) gives the result.

□

Lemma 3.8. *Under the assumptions of Lemma 3.7, there exists a constant such that, for any* dof *and any direction* k*:*

$$\|\bar{\boldsymbol{\omega}}_{k,dof}\| \leq \frac{C_{3.7}}{\sigma^s_{dof} h + \varepsilon}.$$

Proof. We use Lemma 3.7 and $\|\boldsymbol{\omega}_k\| \leq 1$ in (18). This gives:

$$\|\bar{\boldsymbol{\omega}}_{k,\mathrm{dof}}\| \leq \max(1, C_{3.6}) \frac{\varepsilon + \sigma^s_{\mathrm{dof}} h}{(\sigma^s_{\mathrm{dof}} h)^2 + \varepsilon^2} \leq 2 \max(1, C_{3.6}) \frac{1}{\sigma^s_{\mathrm{dof}} h + \varepsilon}. \tag{39}$$

The result is proved.

□

Lemma 3.9. *Under the assumptions of Lemma 3.7, there exists a constant such that:*

$$\|\bar{M}\| \leq \frac{C_{3.8}}{\min_{1 \leq j \leq J} \left(\sigma^s_j\right) h^2 + \varepsilon h}. \tag{40}$$

Proof. Using Lemmas 3.8 and 6.3 gives the result. □

Lemma 3.10. *Under the assumptions of Lemma 3.7, if*

$$\frac{\varepsilon^2 \Delta t}{\varepsilon^2 + \min_{j \in \mathcal{T}}(\sigma^t_j) \Delta t} \frac{C_{3.8}}{\min_{j \in \mathcal{T}}(\sigma^s_j) h^2 + \varepsilon h} < \frac{1}{2}, \tag{41}$$

then:

$$\left\| \left[i_{JK} + \Delta t \mu^{(1)} \bar{M} \right]^{-1} \right\| \leq 2. \tag{42}$$

Proof. Using Lemma 3.9 and Assumption (41), we have:

$$\left\| \Delta t \mu^{(1)} \bar{M} \right\| \leq \frac{1}{2}.$$

A classical computation gives the result.

□

Theorem 3.11. *Under the assumptions of Lemma 3.7, if* (41) *is fulfilled and:*

$$\frac{(\Delta t)^2 \min_{j \in \mathcal{T}}(\sigma^s_j)}{\varepsilon^2 + \min_{j \in \mathcal{T}}(\sigma^t_j) \Delta t} \frac{C_{3.8}}{\min_{j \in \mathcal{T}}(\sigma^s_j) h^2 + \varepsilon h} < 1, \tag{43}$$

then the function f defined by (35) *satisfies $\|\nabla f\| < 1$. Therefore f is a contraction mapping and it admits a unique fixed point which is $\left(I^{n+1}_{k,j}\right)_{k,j}$ the solution of* (30)*. Besides the sequence $\left(\left[I^{n+1,l}_{k,j}\right]_{k,j}\right)_{l \in \mathbb{N}}$ defined in* (33) *converges toward this solution as $l \to \infty$.*

Proof. Using (38) and Lemmas 3.9 and 3.10 gives the result. □

Remark 2. *The following condition is sufficient to ensure* (43)*:*

$$\Delta t \leq C \left(\varepsilon h + \min_{j \in \mathcal{T}}(\sigma^s_j) h^2 \right),$$

which is a classical CFL condition for a system with hyperbolic and parabolic terms.
In particular, in the diffusion regime, we see that if $\Delta t = O(h^2)$ then the fixed point procedure converges. Therefore there is no need to use an acceleration procedure.

3.4 Particular cases

In this section we present two particular cases: the streaming scheme obtained by choosing $(\varepsilon, \sigma^t, \sigma^s) = (1, 0, 0)$ and the limit diffusion scheme obtained as $\varepsilon \to 0$.

3.4.1 Free streaming limit

Choosing $\varepsilon = 1$ and $\sigma^t = \sigma^s = 0$ leads to:

$$V_j \frac{I_{k,j}^{n+1} - I_{k,j}^n}{\Delta t} + \left[M\left(\boldsymbol{\omega}_k\right) I_k^{n+1} \right]_j = V_j q_{k,j}. \tag{44}$$

The scheme reads as K decoupled linear systems. The fixed point algorithm converges in one iteration. Moreover, as the velocity field is constant, the inverse of $i_J + \Delta t M\left(\boldsymbol{\omega}_k\right)$ is not only with nonnegative coefficients but it is also stochastic. Therefore the maximum principle is unconditionally ensured at each iteration.

3.4.2 Diffusion limit

We recall here the limit scheme (32):

$$V_j \frac{E_j^{n+1} - E_j^n}{\Delta t} + \left[M\left(\frac{1}{3\sigma^s}\mathbf{u}^n\right) E^{n+1} \right]_j = V_j \frac{1}{K} \sum_{k'=1}^{K} q_{k',j}. \tag{45}$$

This scheme is first order consistent, unconditionally positive and partially implicit. It is an implicit version of the first order scheme from [20]. However, System (45) is not solved directly. Indeed, due to the fixed-point strategy, E^{n+1} in System (45) is computed as the limit of the following sequence:

$$V_j \frac{E_j^{n+1,l+1} - E_j^n}{\Delta t} + \left[M\left(\frac{1}{3\sigma^s}\mathbf{u}^n\right) E^{n+1,l} \right]_j = V_j \frac{1}{K} \sum_{k'=1}^{K} q_{k',j}. \tag{46}$$

3.5 Summary of the method

We summarize here our scheme:

- compute the average E^n;
- compute the discrete gradients $\left(\mathbf{u}_{\text{dof}}\right)_{\text{dof}\in\mathcal{T}}$ defined in (19) and the velocities $\left(\bar{\boldsymbol{\omega}}_{k,\text{dof}}\right)_{\text{dof}\in\mathcal{T}}$ defined in (18);
- use the fixed-point procedure. Set $I_{k,j}^{n+1,l=0} = I_{k,j}^n$ and iterate Equation (33) until the following condition is fulfilled:

$$\max_{j\in\mathcal{T}} \max_{1\leq k\leq K} \left| I_{k,j}^{n+1,l+1} - I_{k,j}^{n+1,l} \right| \leq 10^{-8}.$$

4 Second order scheme

4.1 Method

In this Section we present a second order scheme. This scheme is not an extension of the scheme from Section 3. Indeed, the streaming term is chosen completely explicit whilst the source terms are still implicit:

$$\frac{I_{k,j}^{n+1} - I_{k,j}^n}{\Delta t} + \mathcal{R}_j(I_k^n, \bar{\boldsymbol{\omega}}_k^n) + \frac{\sigma_j^t}{\varepsilon^2} I_{k,j}^{n+1} = \frac{\sigma_j^s}{\varepsilon^2} \frac{1}{K} \sum_{k'=1}^{K} I_{k',j}^{n+1} + q_{k,j}. \tag{47}$$

The quantity $\mathcal{R}_j(I_k^n, \bar{\boldsymbol{\omega}}_k^n)$ is a second order approximation of

$$\frac{1}{V_j} \int_{\partial\Omega_j} I\bar{\boldsymbol{\omega}}_k. \tag{48}$$

Its definition and properties are detailed in Section 6.2 and we do not recall them here in order to make the algebra clearer. Note that the scheme (47) is conservative:

Proposition 4.1. *We assume periodic boundary conditions are imposed. If $\sigma_j^t = \sigma_j^s$ and $q = 0$, then the scheme* (47) *is conservative:*

$$\sum_{j\in\mathcal{T}} V_j E_j^{n+1} = \sum_{j\in\mathcal{T}} V_j E_j.$$

Proof. As for Proposition 3.1, this result is a direct consequence of Proposition 6.1. □

Besides, owing to Sherman-Morrison Lemma 4.2, we can write an explicit formula for $I_{k,j}^{n+1}$ (Proposition 4.3).

Lemma 4.2. *Let $p \in \mathbb{N}$ and $A \in \mathbb{R}^{p\times p}$, $u \in \mathbb{R}^p$, $v \in \mathbb{R}^p$. The matrix $A + u \otimes v$ is nonsingular if and only if $1 + \langle v, A^{-1}u\rangle \neq 0$. Besides, in this case, its inverse is given by:*

$$(A + u \otimes v)^{-1} = A^{-1} - \frac{1}{1 + \langle v, A^{-1}u\rangle} A^{-1}u \otimes vA^{-1}.$$

Proof. The proof can be found in [22]. □

Proposition 4.3. *Equation* (47) *is equivalent to:*

$$I_{k,j}^{n+1} = \mu_j^{(1)} \left(I_k^n - \Delta t \mathcal{R}_j(I_k^n, \bar{\boldsymbol{\omega}}_k^n)\right) + \mu_j^{(2)} \frac{1}{K} \sum_{k'=1}^{K} \left(I_k^n - \Delta t \mathcal{R}_j(I_k^n, \bar{\boldsymbol{\omega}}_k^n)\right) \tag{49}$$

$$+\Delta t \left(\mu_j^{(1)} q_{k,j} + \mu_j^{(2)} \frac{1}{K} \sum_{k'=1}^{K} q_{k',j}\right),$$

where $\mu_j^{(1)}, \mu_j^{(2)}$ are defined in (26).

Proof. Using (26), Equation (47) reads as:

$$I_{k,j}^{n+1} - \frac{\Delta t \sigma_j^s}{\varepsilon^2 + \Delta t \sigma_j^t} \frac{1}{K} \sum_{k'=1}^{K} I_{k',j}^{n+1} = \mu_j^{(1)} \left(I_k^n - \Delta t \mathcal{R}_j(I_k^n, \bar{\boldsymbol{\omega}}_k^n) + \Delta t q_{k,j}\right). \tag{50}$$

Using Lemma 4.2, Equation (50) becomes:

$$I_{k,j}^{n+1} = \mu_j^{(1)} \left(I_k^n - \Delta t \mathcal{R}_j(I_k^n, \bar{\boldsymbol{\omega}}_k^n) + \Delta t q_{k,j}\right) + \mu_j^{(1)} \frac{\Delta t \sigma_j^s}{\varepsilon^2 + \Delta t(\sigma_j^t - \sigma_j^s)} \frac{1}{K} \sum_{k'=1}^{K} \left(I_k^n - \Delta t \mathcal{R}_j(I_k^n, \bar{\boldsymbol{\omega}}_k^n) + \Delta t q_{k',j}\right). \tag{51}$$

Collecting (26) and (51) gives (49).

□

We see that, if $q = 0$ and $\sigma_j^t = \sigma_j^s$ then $\mu_j^{(1)} + \mu_j^{(2)} = 1$ and $I_{k,j}^{n+1}$ simply reads as a convex combination between the anisotropic and isotropic dynamics. We observe in Section 5 that the scheme (49) is indeed second order convergent. Moreover, the positivity of the solution is preserved under a classical CFL condition:

Proposition 4.4. *Under Assumptions* (9) (10) (11)*, there exists a constant $C > 0$ independent from h, I, σ^s, σ^t, ε and q such that if $\left(I_{k,j}^n\right)_{k,j}$ and q are nonnegative (resp positive), and if:*

$$\Delta t \leq C \left(\min_{j\in\mathcal{T}} \left(\sigma_j^s\right) h^2 + \varepsilon h\right), \tag{52}$$

then the $\left(I_{k,j}^{n+1}\right)_{k,j}$ are nonnegative (resp positive).

Proof. Using $q \geq 0$ and Lemmas 3.8 and 6.5 gives the result. □

Remark 3. *The condition* (52) *is not very restrictive. Indeed, as the scheme* (49) *is first order consistent in time, we need to set $\Delta t = O(h^2)$ in order to make the consistency error decrease as h^2.*

4.2 AP property and limit scheme

In this Section, we explain why the scheme (49) is AP. Choosing $\varepsilon = 0$ in (49) leads to:

$$\frac{E_j^{n+1} - E_j^n}{\Delta t} + \mathcal{R}_j\left(E^n, \frac{1}{3\sigma^s}\mathbf{u}^n\right) = \frac{1}{K}\sum_{k'=1}^{K} q_{k',j}. \tag{53}$$

As $\mathbf{u}$ is a consistent approximation of $-\nabla E/E$, the scheme (53) is consistent with (6). This scheme is the second order scheme from [20].

5 Numerical results

In this Section we present some numerical examples to illustrate the good properties of our method. In the first three test cases, we compute analytical solutions of (2) and we perform a convergence analysis (Sections 5.1, 5.2, 5.3) on cartesian meshes (uniform grids) and random meshes (see Figure 4). Denoting by $\tilde{I}$ the exact solution and T the final time, the error is computed the following way:

$$\text{error} \;=\; \max_{1\leq k\leq K}\left(\frac{\sum_{j\in\mathcal{T}} V_j \left|I_{k,j} - \tilde{I}(t,\mathbf{x}_j,\boldsymbol{\omega}_k)\right|}{\sum_{j\in\mathcal{T}} V_j \tilde{I}(T,\mathbf{x}_j,\boldsymbol{\omega}_k)}\right).$$

We also compute the solution of a *Lattice problem* defined in [23] in Section 5.4.

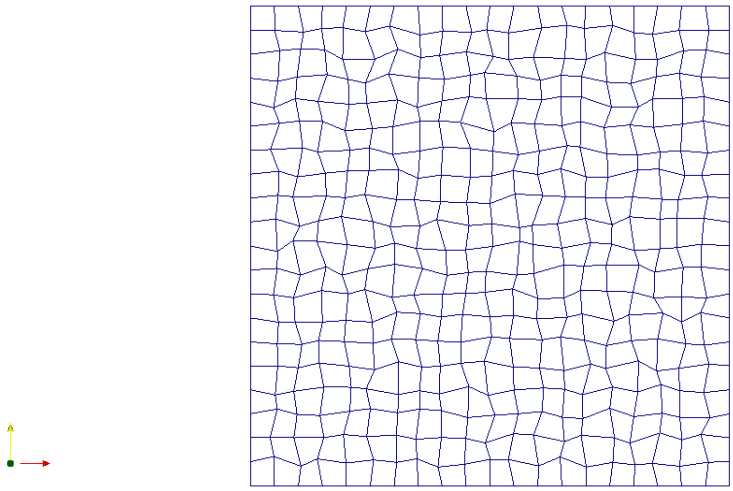

Figure 4: Random mesh.

5.1 Free streaming regime

In this test case, we choose $\sigma^s = \sigma^t = 0$, $q = 0$ and $\varepsilon = 1$. The exact solution is given by:

$$I(t,\mathbf{x},\boldsymbol{\omega}) = \exp\left(-100\left\|\mathbf{x} - t\boldsymbol{\omega} - \mathbf{x}_0\right\|^2\right), \qquad \mathbf{x}_0 = (1,1).$$

Dirichlet boundary conditions are imposed (see Section 6.3). We choose $N = 1$ directions ($K = 4$). The computational domain is $\Omega = [0,2]^2$. We set $\theta = 1$. Figure 5 shows the error curve for the first order scheme, at final time $T = 0.5$ and $\Delta t = h$. Figure 6 shows the error curve for the second order scheme, at final time $T = 0.03$ and $\Delta t = h^2$. We see that our method gives the expected rate of convergence.

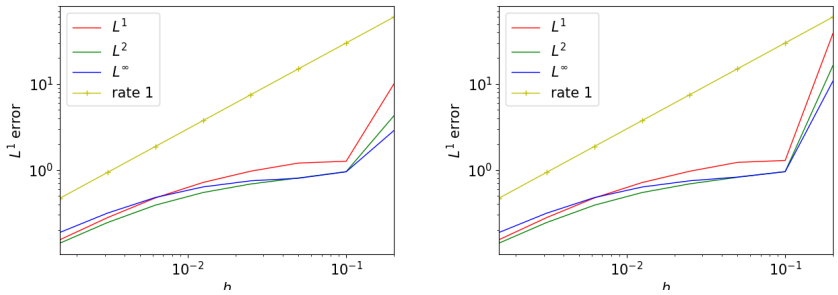

Figure 5: Error with the first order scheme of Section 3 on cartesian (left) and random (right) meshes.

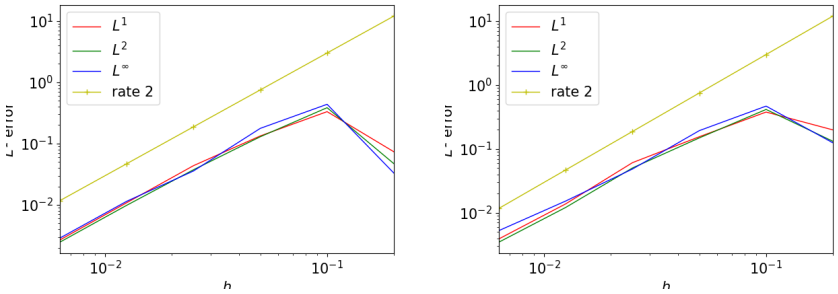

Figure 6: Error with the second order scheme of Section 4 on cartesian (left) and random (right) meshes.

5.2 Diffusion regime

In this test case, we choose $\sigma^s = \sigma^t = 1$, $q = 0$ and $\varepsilon = 0$. The exact solution is the fundamental solution of the diffusion equation:

$$\partial_t E - \frac{1}{3}\Delta E = 0, \qquad E(t, \mathbf{x}) = \frac{3}{4\pi(t+t_0)} \exp\left(-3\frac{\|\mathbf{x}-\mathbf{x}_0\|^2}{4(t+t_0)}\right),$$

with $t_0 = 0.01$ and $\mathbf{x}_0 = (1, 1)$. The computational domain is $\Omega = [0, 2]^2$. Dirichlet boundary conditions are imposed. We choose $K = 4$ directions and $\theta = 1/2$. The timestep is given by $\Delta t = h^2$ and the final time is $T = 0.03$. Figure 7 (resp Figure 8) shows the error curves for the first order scheme (resp second order scheme). The right convergence rate is recovered.

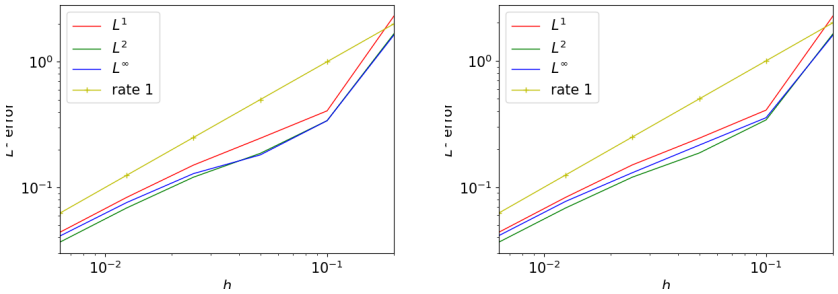

Figure 7: Error with the first order scheme of Section 3 on cartesian (left) and random (right) meshes.

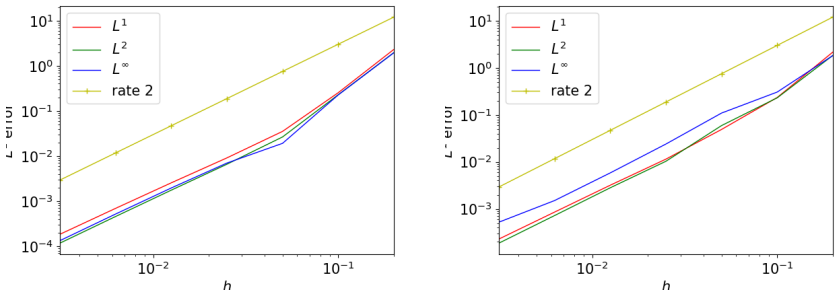

Figure 8: Error with the second order scheme of Section 4 on cartesian (left) and random (right) meshes.

5.3 Manufactured test case

We choose $\varepsilon = 1$. The analytical solution of this test case is given by:

$$I(t, x, y, \boldsymbol{\omega}) = e^t \left(10 + \sin(2\pi x) + \sin(2\pi y) + \langle \boldsymbol{\omega}, \mathbf{f} \rangle\right), \qquad \mathbf{f} = (1, -1),$$

and the absorption coefficients are given by:

$$\sigma^t(x, y) = 2 + (\sin(2\pi x) + \sin(2\pi y))^2, \qquad \sigma^s = 0.1.$$

We compute the source term $q(t, x, y, \boldsymbol{\omega})$ so as to satisfy Equation (2). Periodic boundary conditions are imposed. We set $N = 1$ ($K = 4$). Figure 9 plots the error curves with the first order scheme at time $T = 0.5$ and $\Delta t = h$ and $\theta = 1/2$. Figure 10 displays the error curves with the second order scheme at time $T = 0.01$ and $\Delta t = h^2$ and $\theta = 1/2$.

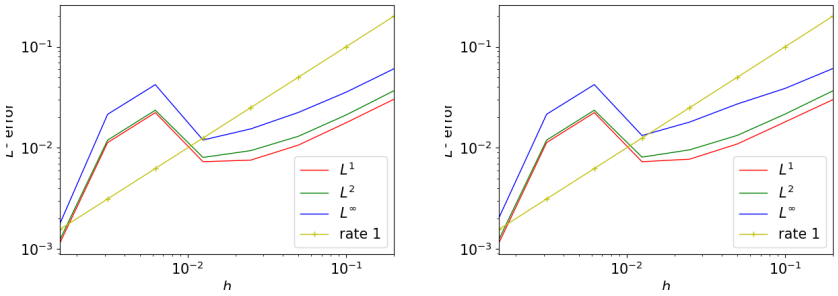

Figure 9: Error with the first order scheme of Section 3 on cartesian meshes (left) and random meshes (right).

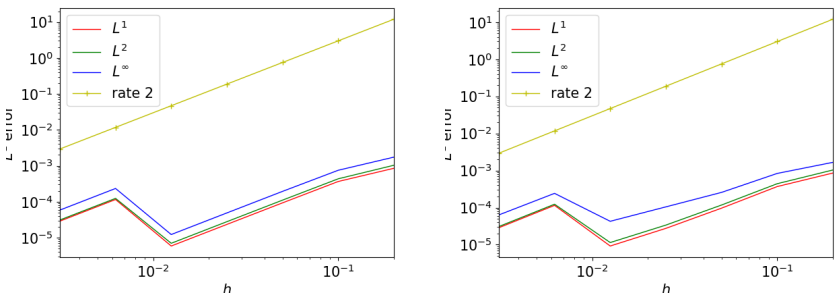

Figure 10: Error with the second order scheme of Section 4 on cartesian meshes (left) and random meshes (right).

5.4 Lattice problem

This test case is borrowed from [23]. The computational domain is $\Omega = [0,7]^2$. The initial condition is 0 and $\varepsilon = 1$. The source term is $q = 1_{[3,4]\times[3,4]}$. Homogeneous Dirichlet boundary conditions are imposed. We set $\theta = 1$. The final time is $T = 3.2$ and the time step is $\Delta t = 0.01$. The absorption coefficients are:

$$\sigma^t(\mathbf{x}) = \begin{cases} 10 & \text{if } \mathbf{x} \in \Omega_A, \\ 5.5 & \text{if } \mathbf{x} \in \partial\Omega_A, \\ 1 & \text{else,} \end{cases} \qquad \sigma^s(\mathbf{x}) = \begin{cases} 0 & \text{if } \mathbf{x} \in \Omega_A, \\ 0.5 & \text{if } \mathbf{x} \in \partial\Omega_A, \\ 1 & \text{else.} \end{cases}$$

The domain Ω_A is pictured in red color in Figure 11.

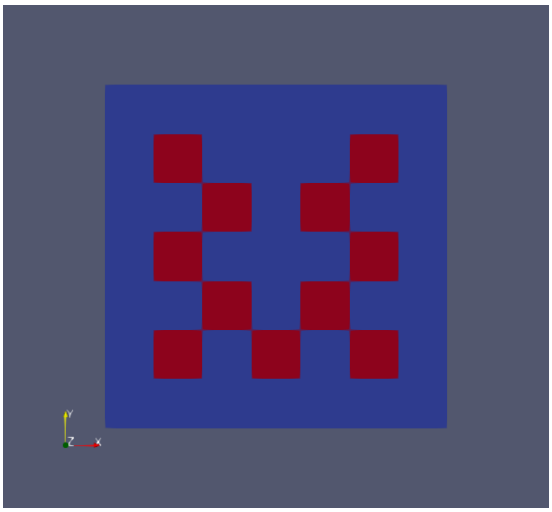

Figure 11: The domain Ω_A in red color.

Some numerical solutions are plotted in the following Figures. The log scale map is limited to seven orders of magnitude: we display with the same blue color all the regions where the solution is smaller or equal to 10^{-7}.

Figures 12 plots the numerical solution computed with the first order scheme of Section 3 with $K = 4$. Figures 13, 14 and 15 display the numerical solution computed with the second order explicit scheme of Section 4 with $K = 4$, $K = 144$ and $K = 484$ respectively. We see that we recover the results of [23].

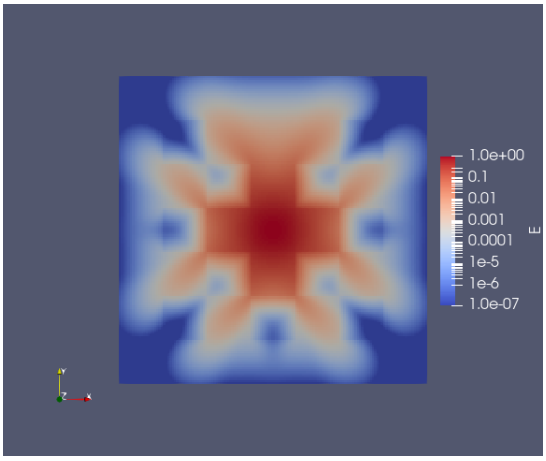

Figure 12: Numerical solution (in log scale) at time $T = 3.2$ computed with the first order scheme of Section 3 on a cartesian mesh of size 140×140 and with $N = 1$ ($K = 4$).

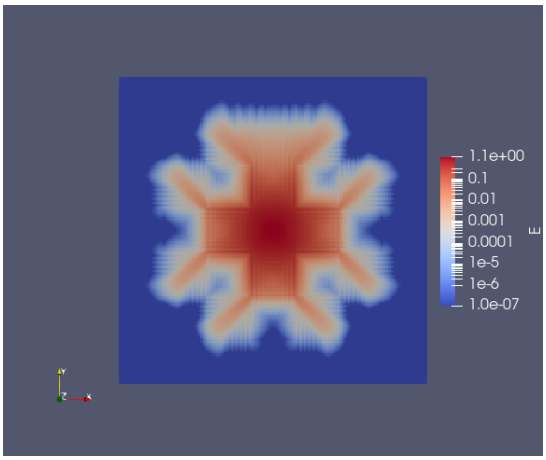

Figure 13: Numerical solution (in log scale) at time $T = 3.2$ computed with the second order scheme of Section 4 on a cartesian mesh of size 140×140 and with $N = 1$ ($K = 4$).

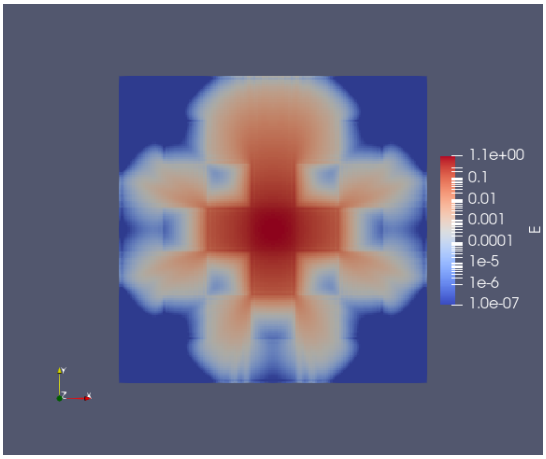

Figure 14: Numerical solution (in log scale) at time $T = 3.2$ computed with the second order scheme of Section 4 on a cartesian mesh of size 140×140 and with $N = 6$ ($K = 144$).

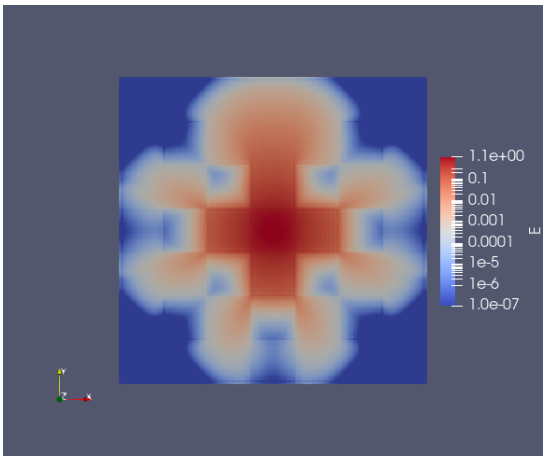

Figure 15: Numerical solution (in log scale) at time $T = 3.2$ computed with the second order scheme of Section 4 on a cartesian mesh of size 140×140 and with $N = 11$ ($K = 484$).

6 Appendix: upwind scheme

In this Section, we present two approximations of $\int_{\partial\Omega_j} g\langle \mathbf{a}, \mathbf{n}\rangle$, where $\mathbf{n}$ is the outward unit vector to $\partial\Omega_j$, g is a given function and $\mathbf{a}$ is a given velocity field. The first one is a classical upwind scheme where the flux is computed at the nodes and at the edges. It is first order consistent. We present it in Section 6.1. Then we propose an extension that is second order consistent in Section 6.2. Eventually we present in Section 6.3 (resp Section 6.4) a way of discretising Dirichlet (resp periodic) boundary conditions.

First we use Theorem 2.2 and we approximate:

$$\int_{\partial\Omega_j} g\langle \mathbf{a}, \mathbf{n}\rangle \approx \theta \sum_{r\in j} \left\langle \mathbf{a}_r, \mathbf{C}_j^r \right\rangle g_{j,r} + (1-\theta) \sum_{r+1/2\in j} \left\langle \mathbf{a}_{r+1/2}, \mathbf{C}_j^{r+1/2} \right\rangle g_{j,r+1/2}, \tag{54}$$

where $\mathbf{a}_{\rm dof} = \mathbf{a}(\mathbf{x}_{\rm dof})$ and $g_{j,\rm dof}$ is an approximation to $(\mathbf{x}_{\rm dof})$ in cell j. It is given by an upwind scheme:

$$g_{j,\rm dof} = \begin{cases} \bar{g}_j^{\rm dof} & \text{if } \langle \mathbf{a}_{\rm dof}, \mathbf{C}_j^{\rm dof}\rangle > 0, \\ \dfrac{1}{\sum_{i\in\mathcal{A}_{\rm dof}^+} \langle \mathbf{a}_{\rm dof}, \mathbf{C}_i^{\rm dof}\rangle} \displaystyle\sum_{i\in\mathcal{A}_{\rm dof}^+} \langle \mathbf{a}_{\rm dof}, \mathbf{C}_i^{\rm dof}\rangle \bar{g}_i^{\rm dof} & \text{else,} \end{cases} \tag{55}$$

where: $\mathcal{A}_{\rm dof}^+ = \{i, \langle \mathbf{a}_{\rm dof}, \mathbf{C}_i^{\rm dof}\rangle > 0\}$. The quantity $\bar{g}_j^{\rm dof}$ is an approximation of g at point $\mathbf{x}_{\rm dof}$ in cell j that is given below. This scheme is conservative:

Proposition 6.1. *We assume that periodic boundary conditions are imposed on g, then the scheme* (54) (55) *is conservative:*

$$\sum_{j\in\mathcal{T}} \left(\theta \sum_{r\in j} \left\langle \mathbf{a}_r, \mathbf{C}_j^r \right\rangle g_{j,r} + (1-\theta) \sum_{r+1/2\in j} \left\langle \mathbf{a}_{r+1/2}, \mathbf{C}_j^{r+1/2} \right\rangle g_{j,r+1/2} \right) = 0.$$

Proof. The proof is given in [12]. □

6.1 First order upwind scheme

We set:

$$\bar{g}_j^{\rm dof} = g_j, \tag{56}$$

then the numerical flux (54)-(55) depends linearly on the $(g_i)_{i\in\mathcal{T}}$. Therefore we write:

$$\theta \sum_{r\in j} \langle \mathbf{a}_r, \mathbf{C}_j^r \rangle \, g_{j,r} + (1-\theta) \sum_{r+1/2\in j} \left\langle \mathbf{a}_{r+1/2}, \mathbf{C}_j^{r+1/2} \right\rangle g_{j,r+1/2} = [M(\mathbf{a})g]_j,$$

where the streaming matrix is defined by:

$$\begin{aligned}(M(\mathbf{a}))_{jl} = 1_{j=l} \Bigg[&(1-\theta) \sum_{r\in R_j^+} \langle \mathbf{a}_r, \mathbf{C}_j^r \rangle + \theta \sum_{r+1/2\in \tilde{R}_j^+} \left\langle \mathbf{a}_{r+1/2}, \mathbf{C}_j^{r+1/2} \right\rangle \Bigg] \\ &+(1-\theta) \sum_{r\in\Omega_j\cap\Omega_l} 1_{r\in R_j^-} \langle \mathbf{a}_r, \mathbf{C}_j^r \rangle \, 1_{l\in\mathcal{A}_r^+} \frac{\langle \mathbf{a}_r, \mathbf{C}_l^r \rangle}{\sum_{i\in\mathcal{A}_r^+} \langle \mathbf{a}_r, \mathbf{C}_i^r \rangle} \\ &+\theta \sum_{r+1/2\in\Omega_j\cap\Omega_l} 1_{r+1/2\in\tilde{R}_j^+} \left\langle \mathbf{a}_{r+1/2}, \mathbf{C}_j^{r+1/2} \right\rangle,\end{aligned} \tag{57}$$

where:

$$R_j^+ = \{r, \langle \mathbf{C}_j^r, \mathbf{a}_r \rangle > 0\}, \qquad R_j^- = \{r, \langle \mathbf{C}_j^r, \mathbf{a}_r \rangle \le 0\},$$

and:

$$\tilde{R}_j^+ = \{r+1/2, \langle \mathbf{C}_j^{r+1/2}, \mathbf{a}_{r+1/2} \rangle > 0\}, \qquad \tilde{R}_j^- = \{r+1/2, \langle \mathbf{C}_j^{r+1/2}, \mathbf{a}_{r+1/2} \rangle \le 0\}.$$

Proposition 6.2. *We assume periodic boundary conditions are imposed on g, then the matrix $M(\mathbf{a})^T$ is an M-matrix.*

Proof. This property is a direct consequence of the conservation property. First, according to (57), we already have:

$$(M(\mathbf{a}))_{jj} \ge 0, \qquad \text{and } j \ne l \quad \Longrightarrow \quad (M(\mathbf{a}))_{jl} \le 0.$$

Moreover, due to the conservation property 6.1, we have:

$$(1,\dots,1) M(\mathbf{a}) g = \sum_{j\in\mathcal{T}} \left(\theta \sum_{r\in j} \langle \mathbf{a}_r, \mathbf{C}_j^r \rangle \, g_{j,r} + (1-\theta) \sum_{r+1/2\in j} \left\langle \mathbf{a}_{r+1/2}, \mathbf{C}_j^{r+1/2} \right\rangle g_{j,r+1/2} \right) = 0. \tag{58}$$

Equation (58) is true for any vector g, therefore leading to:

$$M(\mathbf{a})^T \begin{pmatrix} 1 \\ \vdots \\ 1 \end{pmatrix} = 0.$$

The sum of each line of $M(\mathbf{a})^T$ is 0. Using Proposition 3.4 gives the result.

□

We conclude this Section by giving a useful Lemma:

Lemma 6.3. *Under Assumption* (9)*, there exists a constant such that:*

$$\|M(\mathbf{a})\| \le Ch \|\mathbf{a}\|_{L^\infty(\Omega)}.$$

Proof. We easily have:

$$\left|\sum_{r\in R_j^+}\left\langle \mathbf{a}_r, \mathbf{C}_j^r\right\rangle\right| + \left|\sum_{r+1/2\in \tilde{R}_j^+}\left\langle \mathbf{a}_{r+1/2}, \mathbf{C}_j^{r+1/2}\right\rangle\right| \leq Ch\|\mathbf{a}\|_{L^\infty(\Omega)}, \tag{59}$$

$$\left|\frac{\langle \mathbf{a}_r, \mathbf{C}_l^r\rangle}{\sum_{i\in\mathcal{A}_r^+}\langle \mathbf{a}_r, \mathbf{C}_i^r\rangle}\right| \leq 1, \qquad \left|\sum_{r\in\Omega_j\cap\Omega_l} 1_{r\in R_j^-}\left\langle \mathbf{a}_r, \mathbf{C}_j^r\right\rangle 1_{l\in\mathcal{A}_r^+}\frac{\langle \mathbf{a}_r, \mathbf{C}_l^r\rangle}{\sum_{i\in\mathcal{A}_r^+}\langle \mathbf{a}_r, \mathbf{C}_i^r\rangle}\right| \leq Ch\|\mathbf{a}\|_{L^\infty(\Omega)}, \tag{60}$$

$$\left|\sum_{r+1/2\in\Omega_j\cap\Omega_l} 1_{r+1/2\in\tilde{R}_j^+}\left\langle \mathbf{a}_{r+1/2}, \mathbf{C}_j^{r+1/2}\right\rangle\right| \leq Ch\|\mathbf{a}\|_{L^\infty(\Omega)}. \tag{61}$$

Collecting (59)-(60)-(61) gives:

$$|(M(\mathbf{a}))_{jl}| \leq Ch\|\mathbf{a}\|_{L^\infty(\Omega)}, \tag{62}$$

for any $(j,l)\in[1,J]^2$. Besides, if j and l do not share a node or an edge, then $(M(\mathbf{a}))_{jl}=0$. Therefore the number of non zero entries in line j of the matrix $M(\mathbf{a})$ is $O(1)$. This leads to:

$$\sum_{l=1}^{J}|(M(\mathbf{a}))_{jl}| \leq Ch\|\mathbf{a}\|_{L^\infty(\Omega)}.$$

Using Lemma 6.4 concludes the proof.

□

Lemma 6.4. *Let $A\in\mathbb{R}^{p\times p}$, then:*

$$\|A\| = \max_{U\neq 0}\frac{\|AU\|}{\|U\|} \leq \max_{1\leq l\leq p}\sum_{l'=1}^{p}|A_{l,l'}|.$$

6.2 Second order scheme

We propose here a version of the scheme (54)-(55) that is second order consistent. To this aim, we set:

$$\bar{g}_j^{\text{dof}} = \begin{cases} g_j - \langle \mathbf{p}_{\text{dof}}, \mathbf{x}_j - \mathbf{x}_{\text{dof}}\rangle & \text{if } |\langle \mathbf{p}_{\text{dof}}, \mathbf{x}_j - \mathbf{x}_{\text{dof}}\rangle| < g_j, \\ g_j & \text{else.}\end{cases} \tag{63}$$

The vector $\mathbf{p}_{\text{dof}}$ is an approximation of $-\nabla g$ at point $\mathbf{x}_{\text{dof}}$ computed as:

$$\mathbf{p}_r = \beta_r^{-1}\sum_{i|r\in\Omega_i} g_i\mathbf{C}_i^r, \qquad \mathbf{p}_{r+1/2} = \frac{\mathbf{p}_r + \mathbf{p}_{r+1}}{2} \tag{64}$$

Eventually, we define the second order flux by:

$$\mathcal{R}_j(g,\mathbf{a}) = \frac{\theta}{V_j}\sum_{r\in j}\left\langle \mathbf{a}_r, \mathbf{C}_j^r\right\rangle g_{j,r} + \frac{1-\theta}{V_j}\sum_{r+1/2\in j}\left\langle \mathbf{a}_{r+1/2}, \mathbf{C}_j^{r+1/2}\right\rangle g_{j,r+1/2}, \tag{65}$$

and where $g_{j,\text{dof}}$ is given by (55) (63) (64). Moreover, the positivity property is still valid:

Lemma 6.5. *Under Assumption* (9)*, there exists a constant $C>0$ independent from h, $\mathbf{a}$ and g such that, if $g\geq 0$, and if*

$$\Delta t \leq C\frac{h}{\|\mathbf{a}\|_{L^\infty(\Omega)}}, \tag{66}$$

then $g_j - \Delta t\mathcal{R}_j(g,\mathbf{a})_j \geq 0$.

Proof. We easily have:

$$g_j - \Delta t \mathcal{R}_j(g, \mathbf{a}) \geq g_j - \frac{\Delta t}{V_j} \left[(1-\theta) \sum_{r \in R_j^+} \left\langle \mathbf{a}_r, \mathbf{C}_j^r \right\rangle \bar{g}_j^r + \theta \sum_{r+1/2 \in \tilde{R}_j^+} \left\langle \mathbf{a}_{r+1/2}, \mathbf{C}_j^{r+1/2} \right\rangle \bar{g}_j^{r+1/2} \right].$$

According to (63), we have $\bar{g}_j^{\text{dof}} \leq 2 g_j$. This leads to:

$$g_j - \Delta t \mathcal{R}_j(g, \mathbf{a}) \geq g_j \left(1 - \frac{\Delta t}{V_j} \left[(1-\theta) \sum_{r \in R_j^+} \left\langle \mathbf{a}_r, \mathbf{C}_j^r \right\rangle + \theta \sum_{r+1/2 \in \tilde{R}_j^+} \left\langle \mathbf{a}_{r+1/2}, \mathbf{C}_j^{r+1/2} \right\rangle \right] \right). \tag{67}$$

Besides, using Assumption (9), we have:

$$\frac{\Delta t}{V_j} \left[(1-\theta) \sum_{r \in R_j^+} \left\langle \mathbf{a}_r, \mathbf{C}_j^r \right\rangle + \theta \sum_{r+1/2 \in \tilde{R}_j^+} \left\langle \mathbf{a}_{r+1/2}, \mathbf{C}_j^{r+1/2} \right\rangle \right] \leq C \Delta t \frac{\|\mathbf{a}\|_{L^\infty(\Omega)}}{h}. \tag{68}$$

Collecting (67) and (68) gives the result.

□

6.3 Dirichlet boundary conditions

We denote by $\gamma \in \mathcal{C}^0(\partial\Omega)$ the Dirichlet boundary condition:

$$g(t, \mathbf{x}) = \gamma, \qquad \text{if } \mathbf{x} \in \partial\Omega, \qquad \text{and } \langle \mathbf{a}(\mathbf{x}), \mathbf{n} \rangle < 0. \tag{69}$$

On the boundary of the domain, the vectors $\left(\mathbf{C}_j^{r+1/2}\right)_{j,r+1/2}$ are aligned with the normal vector to the boundary of the domain $\mathbf{n}$. This is not the case for the vectors $\left(\mathbf{C}_j^r\right)_{j,r}$. Thus we need to set $\theta = 1$ to correctly discretise (69).
Besides, in the cells on the boundary and for the edges on the boundary, we set:

$$g_{j,r+1/2} = \begin{cases} \bar{g}_j^{r+1/2}, & \text{if } \langle \mathbf{a}_{r+1/2}, \mathbf{C}_j^{r+1/2} \rangle > 0, \\ \gamma(\mathbf{x}_{r+1/2}) & \text{else,} \end{cases} \tag{70}$$

where $\bar{g}_j^{r+1/2}$ can be computed with the first order method (Section 6.1) or the second order method (Section 6.2).

Note that the gradients $\mathbf{u}_r$ given by (19) is not well-defined in the corner nodes. Indeed there is only one support cell and thus the matrix β_r (8) has rank 1 and is singular. To overcome this difficulty we compute the gradient $\mathbf{u}_r$ at the corner as the average of the gradients at the other nodes of the support cell.

Remark 4. *In the diffusion regime, the Dirichlet boundary condition is imposed on the whole boundary, thus it is no longer necessary to set $\theta = 1$.*

6.4 Periodic boundary conditions

In the case of periodic boundary conditions, we add some *ghost* cells on the outside of the mesh so as to make it periodic. We then define I on these new cells and we use these values and this new geometric data to compute the $\mathbf{C}_j^{\text{dof}}$ on the boundary of the domain.

7 Appendix: proof of Proposition 3.4

First we recall the Gershgorin lemma, whose proof can be found in [22]:

Lemma 7.1 (Gershgorin Lemma)**.** *Let $A \in \mathbb{R}^{p\times p}$ and λ_A one of its eigenvalues. There exists an index $l \in [1, p]$ such that:*

$$|\lambda_A - A_{l,l}| \leq \sum_{l'=1, l'\neq l}^{p} |A_{l,l'}|.$$

Now we can prove Proposition 3.4. We define $c = \max_{1\leq l\leq p} A_{l,l}$, then A can be written as:

$$A = cI - (cI - A).$$

The matrix $cI - A$ has nonnegative coefficients. We prove that is spectral radius is smaller than c. Its eigenvalues are of the form $c - \lambda_A$ with λ_A an eigenvalue of A. Owing to Lemma 7.1, there exists an index l such that:

$$|c - \lambda_A - (c - A_{l,l})| \leq \sum_{l'=1, l'\neq l}^{p} |A_{l,l'}| = -\sum_{l'=1, l'\neq l}^{p} A_{l,l'}. \tag{71}$$

Therefore, using $c - A_{l,l} \geq 0$, we end up with:

$$|c - \lambda_A| \leq c - A_{l,l} - \sum_{l'=1, l'\neq l}^{p} A_{l,l'}. \tag{72}$$

Besides:

$$-A_{l,l} - \sum_{l'=1, l'\neq l}^{p} A_{l,l'} \leq 0. \tag{73}$$

This leads to $|c - \lambda_A| \leq c$ and this inequality is strict if (24) is strict.

References

[1] Dimitri Mihalas and Barbara Weibel Mihalas. *Foundations of radiation hydrodynamics.* Oxford University Press, New York, 1984.

[2] K.M. Case and P.F. Zweifel. *Linear Transport Theory.* Addison-Wesley series in nuclear engineering. Addison-Wesley Publishing Company, 1967.

[3] Dautray Robert, Lions Jacques-Louis, Artola Michel, Cessenat Michel, Scheurer Bruno, and Robert Dautray. *Analyse mathématique et calcul numérique pour les sciences et les techniques . Volume 8, Évolution, semi-groupe, variationnel / Robert Dautray, Jacques-Louis Lions Michel Artola, Michel Cessenat, Bruno Scheurer.* Collection Enseignement - INSTN CEA. Masson, Paris Milan Barcelone [etc, [nouvelle édition] edition, 1988.

[4] C Bardos, F Golse, B Perthame, and R Sentis. The nonaccretive radiative transfer equations: Existence of solutions and rosseland approximation. *Journal of Functional Analysis*, 77(2):434–460, 1988.

[5] John Castor. *Radiation Hydrodynamics.* Cambridge University Press, 2004.

[6] Edward W larsen and J.E. Morel. Asymptotic solutions of numerical transport problems in optically thick, diffusive regimes ii. *Journal of Computational Physics*, 83(1):212–236, 1989.

[7] Shi Jin and C.David Levermore. Numerical schemes for hyperbolic conservation laws with stiff relaxation terms. *Journal of Computational Physics*, 126(2):449 – 467, 1996.

[8] M.L. Adams. Discontinuous finite element transport solutions in thick diffusive problems. *Nuclear Science and Engineering*, 137(3):298 – 333, 2001.

[9] T S Bailey, J H Chang, J S Warsa, and M L Adams. A piecewise bi-linear discontinuous finite element spatial discretization of the sn transport equation.

[10] F. Chaland and G. Samba. Discrete ordinates method for the transport equation preserving one-dimensional spherical symmetry in two-dimensional cylindrical geometry. *Nuclear Science and Engineering*, 182(4):417–434, 2016.

[11] Christophe Buet, Bruno Després, and Emmanuel Franck. Design of asymptotic preserving finite volume schemes for the hyperbolic heat equation on unstructured meshes. *Numer. Math.*, 122(2):227–278, 2012.

[12] Xavier Blanc, Philippe Hoch, and Clément Lasuen. An asymptotic preserving scheme for the M1 model on conical meshes. working paper or preprint, 2021.

[13] G. Carré, S. Del Pino, B. Després, and E. Labourasse. A cell-centered Lagrangian hydrodynamics scheme on general unstructured meshes in arbitrary dimension. *J. Comput. Phys.*, 228(14):5160–5183, 2009.

[14] Philippe Hoch. Nodal extension of Approximate Riemann Solvers and nonlinear high order reconstruction for finite volume method on unstructured polygonal and conical meshes: the homogeneous case. working paper or preprint, February 2022.

[15] Pierre Anguill, Patricia Cargo, Cedric Énaux, Philippe Hoch, Emmanuel Labourasse, and Gerald Samba. An asymptotic preserving method for the linear transport equation on general meshes. *Journal of Computational Physics*, 450:110859, 2022.

[16] B G Carlson. Transport theory: Discrete ordinates quadrature over the unit sphere.

[17] Lawrence C. Evans. *Partial differential equations*. American Mathematical Society, 2010.

[18] Aude Bernard-Champmartin, Philippe Hoch, and Nicolas Seguin. Stabilité locale et montée en ordre pour la reconstruction de quantités volumes finis sur maillages coniques non-structurés en dimension 2. Research report, CEA, CEA/DAM/DIF, Bruyères-le-Châtel, France ; Univ-Rennes1 ; Université Paris 6, March 2020. `https://hal.archives-ouvertes.fr/hal-02497832`.

[19] Emmanuel Franck. *Construction et analyse numérique de schema asymptotic preserving sur maillages non structurés. Application au transport linéaire et aux systèmes de Friedrichs*. PhD thesis, Université Pierre et Marie Curie - Paris VI, 2012.

[20] Xavier Blanc, Philippe Hoch, and Clément Lasuen. Composite finite volume schemes for the diffusion equation on unstructured meshes. working paper or preprint, October 2023.

[21] R.S. Varga. *Matrix Iterative Analysis*. Springer Series in Computational Mathematics. Springer Berlin Heidelberg, 1999.

[22] Denis Serre. Matrices: Theory and applications. 2002.

[23] Thomas A. Brunner and James Paul Holloway. Two-dimensional time dependent Riemann solvers for neutron transport. *J. Comput. Phys.*, 210(1):386–399, 2005.

[24] Gerald N. Minerbo. Maximum entropy eddington factors. *Journal of Quantitative Spectroscopy and Radiative Transfer*, 20(6):541 – 545, 1978.

[25] C. David Levermore. Moment closure hierarchies for kinetic theories. *J. Statist. Phys.*, 83(5-6):1021–1065, 1996.

[26] Bruno Després. Weak consistency of the cell-centered Lagrangian GLACE scheme on general meshes in any dimension. *Comput. Methods Appl. Mech. Eng.*, 199(41-44):2669–2679, 2010.

[27] Laurent Gosse and Giuseppe Toscani. An asymptotic-preserving well-balanced scheme for the hyperbolic heat equations. *C. R. Math. Acad. Sci. Paris*, 334(4):337–342, 2002.

[28] James M. Greenberg and Alain-Yves Le Roux. A well-balanced scheme for the numerical processing of source terms in hyperbolic equations. *SIAM J. Numer. Anal.*, 33(1):1–16, 1996.

[29] C. Bardos, F. Golse, and B. Perthame. The Rosseland approximation for the radiative transfer equations. *Comm. Pure Appl. Math.*, 40(6):691–721, 1987.

[30] Gerald C. Pomraning. *Linear kinetic theory and particle transport in stochastic mixtures.* Singapore etc.: World Scientific, 1991.

[31] S. Chandrasekhar. *Radiative transfer.* Dover Publications, Inc., New York, 1950.

[32] Emmanuel Franck. *Design and numerical analysis of asymptotic preserving schemes on unstructured meshes. Application to the linear transport and Friedrichs systems.* Theses, Université Pierre et Marie Curie - Paris VI, October 2012.

[33] Laurent Gosse and Giuseppe Toscani. An asymptotic-preserving well-balanced scheme for the hyperbolic heat equations. *Comptes Rendus Mathematique*, 334(4):337 – 342, 2002.

[34] Franck, Emmanuel, Hoch, Philippe, Navaro, Pierre, and Samba, Gérald. An asymptotic preserving scheme for p1 model using classical diffusion schemes on unstructured polygonal meshes. *ESAIM: Proc.*, 32:56–75, 2011.

[35] Bruno Després and Christophe Buet. The structure of well-balanced schemes for Friedrichs systems with linear relaxation. *Appl. Math. Comput.*, 272(part 2):440–459, 2016.

[36] Christophe Buet, Bruno Després, Emmanuel Franck, and Thomas Leroy. Proof of uniform convergence for a cell-centered AP discretization of the hyperbolic heat equation on general meshes. *Math. Comp.*, 86(305):1147–1202, 2017.

[37] Christophe Buet, Bruno Després, and Emmanuel Franck. Asymptotic preserving schemes on distorted meshes for Friedrichs systems with stiff relaxation: application to angular models in linear transport. *J. Sci. Comput.*, 62(2):371–398, 2015.

[38] Jérôme Breil and Pierre-Henri Maire. A cell-centered diffusion scheme on two-dimensional unstructured meshes. *J. Comput. Phys.*, 224(2):785–823, 2007.

[39] Constant Mazeran. *Sur la structure mathématique et l'approximation numérique de l'hydrodynamique lagrangienne bidimensionnelle.* PhD thesis, Université de Bordeaux I, 2007.

[40] Bernard-Champmartin, Aude, Deriaz, Erwan, Hoch, Philippe, Samba, Gerald, and Schaefer, Michael. Extension of centered hydrodynamical schemes to unstructured deforming conical meshes : the case of circles. *ESAIM: Proc.*, 38:135–162, 2012.

[41] Wang Guojin. Computing integral values involving nurbs curves. *Jour. of Software*, 7:542–546, 1998.

[42] Benjamin Boutin, Erwan Deriaz, Philippe Hoch, and Pierre Navaro. Extension of ale methodology to unstructured conical meshes. In *ESAIM: Proc.*, volume 32, pages 31–55, 2011.

[43] Aude Bernard-Champmartin, Erwan Deriaz, Philippe Hoch, Gerald Samba, and Michael Schaefer. Extension of centered hydrodynamical schemes to unstructured deforming conical meshes : the case of circles. In *ESAIM : proc.*, volume 135-162, 2012.

[44] Ryan G. McClarren, James Paul Holloway, and Thomas A. Brunner. Analytic p1 solutions for time-dependent, thermal radiative transfer in several geometries. *Journal of Quantitative Spectroscopy and Radiative Transfer*, 109(3):389 – 403, 2008.

[45] C. Cancès, M. Cathala, and C. Le Potier. Monotone corrections for generic cell-centered finite volume approximations of anisotropic diffusion equations. *Numer. Math.*, 125:387–417, 2013.

[46] Leo Agelas and Roland Masson. Convergence of the finite volume mpfa o scheme for heterogeneous anisotropic diffusion problems on general meshes. *Comptes Rendus Mathematique*, 346(17):1007 – 1012, 2008.